Original Article

Asian Pacific Journal of Tropical Biomedicine

journal homepage: www.apjtb.org

doi: 10.4103/2221-1691.284947

Impact Factor: 1.59

Antibiofilm activity of alpha-mangostin loaded nanoparticles against *Streptococcus mutans*

Phuong T.M. Nguyen[1,2✉], Minh T.H. Nguyen[3], Lien T. Quach[1], Phuong T.M. Nguyen[1], Lam L. Nguyen[3], Dong V. Quyen[1,3]

[1]*Institute of Biotechnology, Vietnam Academy of Science and Technology, 18 Hoang Quoc Viet Road, Hanoi, Vietnam*

[2]*Institute of Graduate University of Science and Technology, Vietnam Academy of Science and Technology, 18 Hoang Quoc Viet Road, Hanoi, Vietnam*

[3]*University of Science and Technology of Hanoi, Vietnam Academy of Science and Technology, 18-Hoang Quoc Viet Road, Cau Giay, Hanoi, Vietnam*

ABSTRACT

Objective: To investigate the antibiofilm activity of alpha-mangostin (AMG) loaded nanoparticle (nanoAMG) against dental caries pathogen *Streptococcus mutans*.

Methods: AMG was isolated from the peels of *Garcinia mangostana* L. using silica gel columns and chemically analysed by high performance liquid chromatography and nuclear magnetic resonance. NanoAMG was prepared using the solvent evaporation method combined with high-speed homogenization. The nanoparticles were characterized using dynamic light scattering, field emission scanning electron microscopy (FE-SEM) and Fourier transform infrared spectroscopy (FTIR). The toxicity of nanoAMG in fibroblast NIH/3T3 cell line was determined using MTT method. The antibiofilm effect of nanoAMG was determined through the evaluation of biofilm formation by *Streptococcus mutans* using a 96-well plate. Biofilm biomass was quantified using crystal violet. Cell viability was observed under confocal microscopy using LIVE/DEAD BacLight staining. Moreover, gene expression was determined by quantitative real-time PCR and membrane permeabilization activity by measuring the uptake of o-nitrophenol-β-*D*-galactoside.

Results: NanoAMG size was in a range of 10-50 nm with a polydispersity index of < 0.3 and zeta potential value of −35.2 mV. The size and the incorporation of AMG in the nanoparticles were confirmed by FE-SEM and FTIR analyses. The IC_{50} values of the test agents on NIH/3T3 cells were (9.80 ± 0.63) μg/mL for AMG and (8.70 ± 0.81) μg/mL for nanoAMG, while no toxicity was generated from excipients used to prepare nanoparticles. In the early stage of biofilm formation, treatment with 6.25 μmol/L nanoAMG caused a reduction in biofilm biomass up to 49.1%, compared to 33.4% for AMG. In contrast, biofilms at the late stage were more resistant to the test agents. At 96 μmol/L (= 10 × MIC), nanoAMG reduced only 20.7% of biofilm biomass while AMG did not show any effect. Expressions of *gtfB* and *gtfC* genes involved in biofilm formation were down-regulated 3.3 and 12.5 folds, respectively, compared to AMG (2.4 and 7.6 folds, respectively). LIVE/DEAD BacLight fluorescence staining and microscopy observation indicated that biofilm cells were killed by both nanoAMG and AMG at 48 μmol/L (= 5 × MIC). In addition, membrane permeabilization activity was increased in a time dependent manner and higher in nanoAMG treated cells compared to AMG.

Conclusions: AMG coated nanoparticle can enhance AMG bioactivity and can be used as a new and promising antibiofilm agent.

KEYWORDS: Alpha-mangostin; Nanoparticle; Antibiofilm activity; *Streptococcus mutans*

1. Introduction

Biofilm-related bacterial infections are common and pose a significant worldwide problem, as they are generally more tolerant to antibiotics than the planktonic form[1-4]. Therefore, novel and safe strategies for battling clinically relevant biofilms are urgently needed. Among strategies for biofilm control, nanoparticle-based

✉To whom correspondence may be addressed. E-mail: phuongnguyenibt@gmail.com

How to cite this article: Nguyen PTM, Nguyen MTH, Quach LT, Nguyen PTM, Nguyen LL, Quyen DV. Antibiofilm activity of alpha-mangostin loaded nanoparticles against *Streptococcus mutans*. Asian Pac J Trop Biomed 2020; 10(7): 325-332.

Article history: Received 12 October 2019; Revision 16 December 2019; Accepted 14 February 2020; Available online 3 June 2020

antibiofilm designs for treating biofilm disease, including dental caries have been recently reported as a promising approach[5–7].

Alpha-mangostin (AMG), a xanthone purified from *Garcinia mangostana* L. (*G. mangostana*), possesses extensive biological activities and pharmacological properties, such as antioxidant, antiproliferation and apoptosis inducer. More recently, it was found to have an effect on the cardiovascular system, free radical oxidation and biofilm formation by *Staphylococcus aureus*, including MRSA strain, *Staphylococcus epidermidis* and *Acinetobacter baumannii*[8–11]. For anticaries activity, it is an effective antimicrobial agent against planktonic cells of *Streptococcus mutans* (*S. mutans*), a major causative agent of dental caries and a strong biofilm producer in dental plaque[12]. AMG also exhibited antibiofilm activity against *S. mutans* through disruption of the development and mechanical stability of biofilms as well as of acidogenicity[13]. However, the potential use of AMG to prevent biofilm formation is a clinical issue due to its low solubility and bioavailability (0.2 μg/mL)[14]. Therefore, in this study, AMG was isolated from pericarps of *G. mangostana* grown in Vietnam and the AMG loaded nanoparticles (nanoAMG) were prepared and used to enhance the bioavailability of AMG and diffusion capacity into biofilm matrix, and consequently, to improve its antibiofilm activity for therapeutic applications.

2. Materials and methods

2.1. Extraction and isolation of AMG

The dried powder of *G. mangostana* peels was collected from the South of Vietnam and the voucher specimen (No. 15062014) was deposited at the Institute of Ecology and Biological Resources, Vietnam Academy of Science and Technology, Hanoi. The extraction and isolation procedures to obtain AMG were done as previously described[9,15]. The purified AMG was identified by ^{1}H and ^{13}C – nuclear magnetic resonance (NMR), mass spectrometry (MS) and high performance liquid chromatography (HPLC).

2.2. Bacteria and growth conditions

S. mutans UA 159 was cultured statically in 3% tryptone, 0.5% yeast extract, and 1% glucose (TYG) medium at 37 ℃. For biofilm assays, the organism was grown in 3% tryptone, 0.5% yeast extract, and 1% sucrose (TYS) at 37 ℃ on a 3-dimensional plate rocking machine.

2.3. Preparation of nanoAMG

AMG loaded polymeric nanoparticle was prepared using Tween 20 (Sigma-Aldrich) and polyethylene glycol (PEG) 400 (Sigma-Aldrich) based on the method described previously by Rachmawati *et al.*[16] with some modifications. Briefly, AMG was dissolved in ethanol, followed by mixing with a magnetic stirrer for 15 min at 100 rpm. Tween 20 was then added and the mixture was stirred for 15 min. PEG 400 was added, followed by constant stirring for 2 h. The resulting solution was sonicated using an ultrasonicator bath for 30 min. Distilled water was added with a ratio of 1:1. Mild stirring was then conducted for a further 30 min to collect homogenous solution.

2.4. Characterization of nanoAMG

The size, polydispersity index, and zeta potential of the final product were measured using a HORIBA SZ-100 analyzer (Germany) and observed under a high-resolution field emission scanning electron microscope (FE-SEM, Hitachi-S4800, Japan). FTIR spectrum of nanoAMG was recorded by Nicolet iS50 FTIR (Thermo Scientific). AMG content in the nanosystem was determined by liquid chromatography-mass spectrometry, using an Agilent 1260 Single Quadrupole LC/MS System and spectrophotometer (Jenway, 7305, UK). AMG (Sigma-Aldrich) was used as a standard.

2.5. In vitro cytotoxicity

Cytotoxicity against fibroblast NIH/3T3 cells of nanoAMG and the blank carrier was determined using 3-(4,5-dimetylthiazol-2-yl)-2,5-diphenyl tetrazolium bromide (MTT) assay. Briefly, the cells were inoculated at a 10 000 cells/well in a 96-well plate in Dulbecco's Modified Eagle's Medium (Gibco) supplemented with 10% fetal bovine serum, 2 μmol/*L*-glutamine, 100 units/mL penicillin and 100 μg/mL streptomycin, grown to sub-confluence for 2 d at 37 ℃ with 5% CO_2 and then incubated with different concentrations of test compounds for 18 h. The cell viability was determined using MTT assay in which MTT (Sigma-Aldrich) was reduced to formazan. MTT (5 mg/mL in phosphate-buffered saline) was added to each well and incubated for 4 h. The formazan crystal was dissolved in dimethyl sulfoxide. The absorbance values of the solutions were measured at 570 nm using a plate reader (Corning Costa). The result was represented as the percentage of cell viability, compared to untreated controls. Analysis and comparison of IC_{50} values of AMG, nanoAMG and blank carrier were performed. The IC_{50} value was calculated by linear regression.

2.6. Minimal inhibitory concentration (MIC)

A modified broth microdilution method according to the Clinical and Laboratory Standard Institute Guidelines[17] was used to determine the MIC values of AMG. Two-fold serial dilutions of AMG were made in TYG using 96-well flat-bottom microtiter plates (Corning Costa). A suspension of mid-logarithmic growth phase bacteria in TYG adjusted to 1×10^{5} cfu/mL was added to each well. The final concentrations of AMG ranged from 1.145 to 36.600 μmol/L. The MIC was the lowest concentration of AMG showing no visible growth of microorganisms after incubation at 37 ℃ for 24 h. The test was repeated in triplicate.

2.7. Antibiofilm assay

S. mutans was cultured overnight in TYS and diluted for biofilm growth in a 96-well polystyrene plate. The plates were incubated for 48 h at 37 ℃ on a 3-dimensional plate rocking machine. Media were freshly replaced after 24 h growth. After growing, the wells were washed twice with phosphate-buffered saline to remove non-adherent bacteria. The biofilms that formed in the wells were then stained with 0.1% crystal violet for 10 min. Excess stain was removed by washing three times with phosphate-buffered saline. The absorbed crystal violet was dissolved in 30% v/v acetic acid and the absorbance was quantified at λ = 595 nm (A_{595})[18]. The mean of the five replicates was calculated after subtraction of the blank measurement and the results were expressed as a percentage of biofilm in relation to the untreated control.

2.8. Reverse transcription-quantitative PCR (qRT-PCR)

qRT-PCR was performed to evaluate the expression of *gtfB* and *gtfC* genes encoding glucosyltransferases (Gtfs) responsible for biofilm synthesis by *S. mutans*. The time point 20 hours biofilm growth was selected based on our biochemical data and previous studies on the dynamics of the *S. mutans* transcriptome during biofilm formation on sHA and in response to topically applied agents[13]. In this experiment, biofilms were grown in 24 well plastic plates (Costar, USA) in the presence of the test agents of 6.25 μmol/L for 20 h. After treatment, biofilms were washed 2 times with 0.9% NaCl and collected for RNA extraction using RNeasy Mini Kit (Qiagen, Stockach, Germany) according to a standard protocol. cDNA was prepared using M-MLV Reverse Transcriptase (Enzynomics, Korea) according to the manufacturer's method.

For gene quantitative real-time PCR, the PCR mixtures (20 μL) contained 1 μL of cDNA, primers (1 μM concentration, Table 1), and 10 μL TOPreal™ qPCR 2× PreMIX (SYBR Green with low ROX) master mix. The replication process involved denaturation step at 95 ℃ for 10 s, followed by 35 cycles of denaturation at 95 ℃ for 15 s, 60 ℃ for 20 s, and 72 ℃ for 20 s. Each measurement was performed in three replicates. Data were analyzed using Bio-Rad CFX manager software and calculation of gene expression levels was normalized to the signal of the reference gene *16S* rRNA. The values were used to determine the fold-change between the treated sample and the untreated control[19].

Table 1. PCR primers sequences.

Genbank ID	Gene	Sequence primer (5'-3')
SMU.1004	*gtfB*	F: AACAACCGAAGCTGATACAG
		R: CAATTTCTTTTACATTGGGAAGT
SMU.1005	*gtfC*	F:CTCTGACTGCTACTGATACAAG
		R: CCGAAGTTGTTGTTGGTTTAAC
X58303.1	*16S* rRNA	F: CTTACCAGAAAGGGACGGCT
		R: TAGCCTTTTACTCCAGACTTTC

F: Forward; R: Reverse.

2.9. Confocal microscopy

Polyvinyl plastic coverslips (22 mm × 22 mm) were sterilized in absolute isopropanol, dried and placed in wells of a 6-well cell culture plate. An aliquot (2 mL) of the diluted bacterial suspension of *S. mutans* in TYS was added. To test inhibition of the formation of biofilms, AMG was added to the wells at the start of biofilm growth. To test the disruption and/or killing of biofilms, biofilms were grown for 24 h, followed by the removal of planktonic cells and the addition of AMG in fresh medium. The coverslips in the 6-well plate were incubated at 37 ℃ for further 24 h. The culture medium was then removed and the coverslips were 3 times washed with sterile water. Subsequently, biofilms were stained with 0.3% v/v LIVE/DEAD BacLight mixture of dye solution. The coverslips were left for 15 min in the dark prior to washing again with sterile water. The coverslips were mounted on glass slides and sealed with nail varnish. Stained biofilms were observed using laser scanning confocal fluorescence microscopy (Olympus, Tokyo, Japan). The image data were processed with the Imaris software (Bitplane AG, Zürich, Switzerland)[20].

2.10. Cytoplasmic membrane permeabilization assay

NanoAMG-induced permeabilization of the cell membrane was determined using o-nitrophenol-β-*D*-galactoside (ONPG, Sigma-Aldrich). Briefly, 50 μL ONPG with either 12.5 μmol/L of AMG or nanoAMG was applied to the wells. Finally, 50 μL of cell suspension (OD = 0.3) was added to the wells to give a final concentration of 100 μg/mL ONPG. After warming to 37 ℃, the plates were positioned in the plate reader at 37 ℃. ONPG uptake and cleavage by β-galactosidase within the cytoplasm was characterized by following absorption over a period of 180 min at 420 nm. Nisin (Sigma-Aldrich) of 0.5 μg/mL served as a positive control and wells without the test agents served as a negative control[21].

2.11. Statistical analysis

Data were presented as mean ± standard deviation (SD). Student's *t*-test was used to calculate the significance of the difference between the mean of experimental and control samples. The level of significance was set at $P < 0.05$.

3. Results

3.1. Isolation of AMG from the peels of G. mangostana

The purity of the AMG compound exceeded 98% as determined by HPLC. ^{1}H and ^{13}C NMR spectra data were measured and interpreted (Supplementary Table). Based on the analysed and reference data[8,22], the chemical structure of AMG (Supplementary Figure) was confirmed with molecular formula of $C_{24}H_{26}O_6$ and molecular weight of 410.459 6.

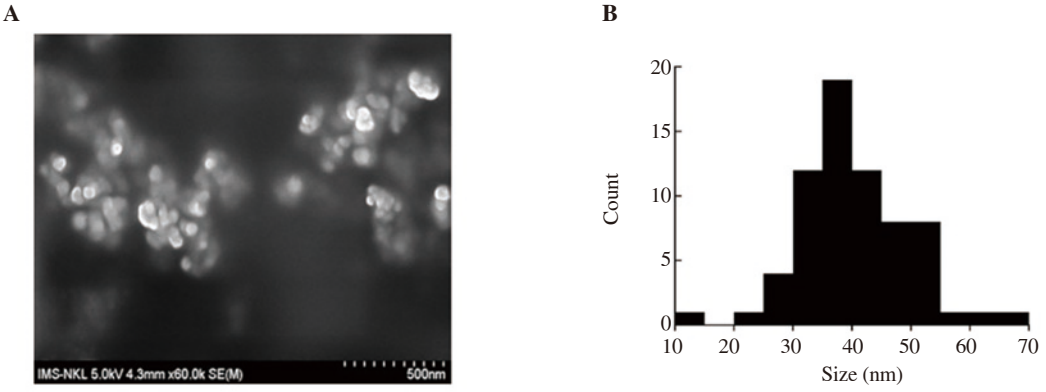

Figure 1. FE-SEM image of nanoAMG at magnification of 60 000× (A) and size distribution histogram of nanoAMG (B) (FE-SEM, Hitachi-S4800, Japan).

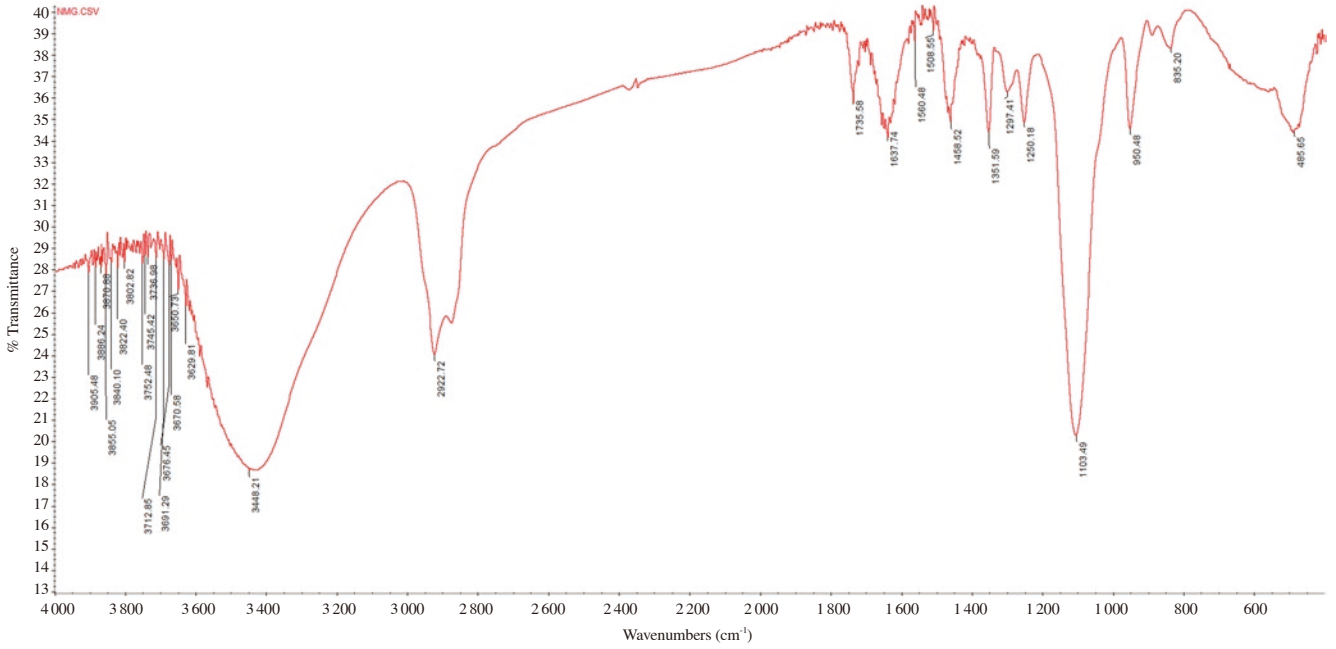

Figure 2. FTIR image of nanoAMG recorded by a FTIR spectrometer (Nicolet iS50 FTIR, Thermo Scientific) with resolution 2 cm^{-1} by scanning 20 times from 400 cm^{-1} to 4 000 cm^{-1} at room temperature.

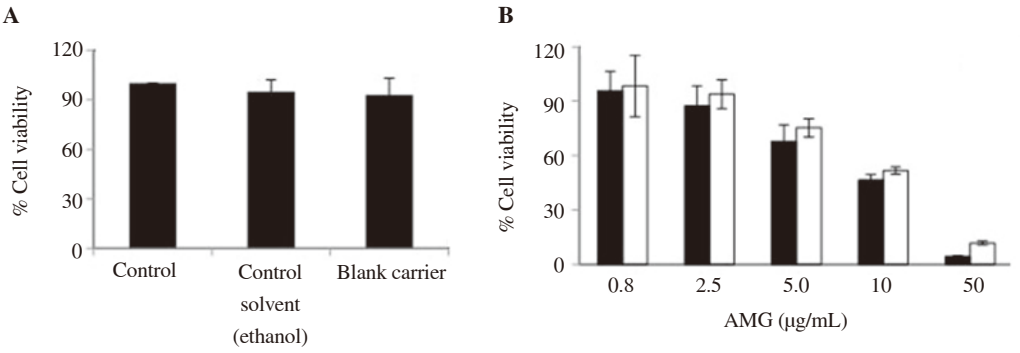

Figure 3. Cell viability of NIH/3T3 cells after treatment with controls (A) and nanoAMG (B). Cell viability was measured using the MTT assay. Student's *t*-test was performed and data were expressed as mean ± SD (n=5). NanoAMG (■); AMG (□).

3.2. Characterization of nanoAMG

The obtained data indicated that the particle size was in a range of 10-50 nm with a polydispersity index of (0.28 ± 0.08) and zeta potential value of −(35.20 ± 0.52) mV. Analysis of nanoparticle morphology by FE-SEM showed the spherical particles of AMG with a size of (40 ± 9) nm (Figure 1). FTIR analysis (Figure 2) confirmed that AMG was incorporated in the nanoparticles.

HPLC determination indicated AMG concentration of the synthesized solution was from 0.3 to 2.4 mg/mL, depending on the amount of loaded AMG (data not shown).

3.3. Cytotoxicity of nanoAMG

A fibroblast NIH/3T3 cell line (NIH/3T3 cells) was exposed to increasing concentrations of nanoAMG for 18 h, and toxicity was analysed using the MTT assay. The IC_{50} values were calculated by linear regression compared to vehicle-treated cells with a concentration of (9.80 ± 0.63) μg/mL for AMG and (8.70 ± 0.81) μg/mL for nanoAMG, while no toxicity was generated from excipients

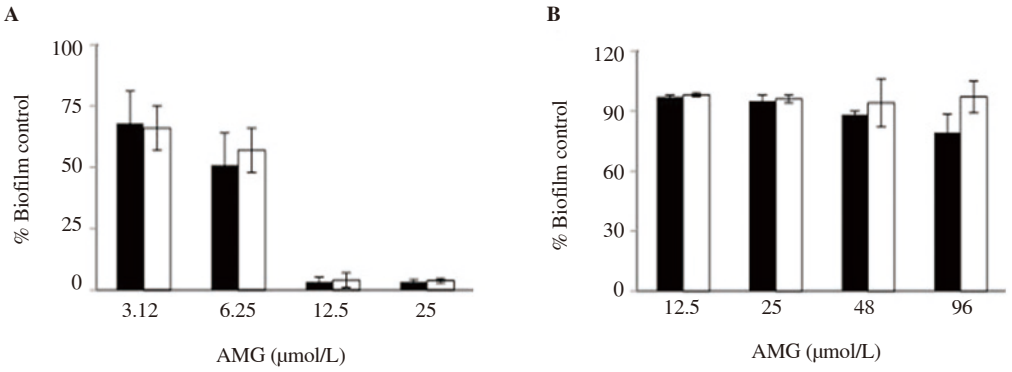

Figure 4. Antibiofilm activity of nanoAMG on biofilm formation by *Streptococcus mutans* at the early stage (A) and late-stage (B). nanoAMG (■); AMG (□). Student's *t*-test was performed and data were expressed as mean ± SD (n=5).

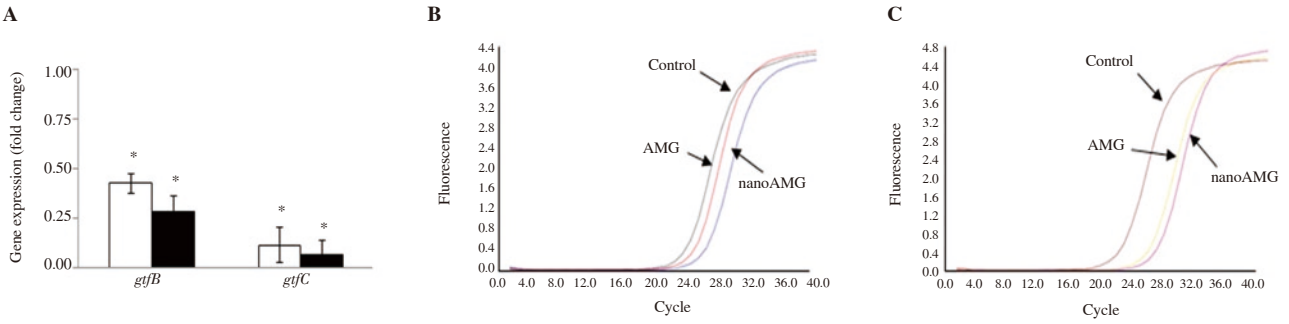

Figure 5. The expression of *Streptococcus mutans* genes *gtfB* and *gtfC* in biofilms (A) and their fluorescence signals at different treatment concentrations of AMG (□) and nanoAMG (■) for *gtfB* (B) and *gtfC* (C). Fold changes ± standard deviation. Values marked with asterisks are significantly different from that for the untreated control (n = 3; $^{*}P$<0.05, pair-wise comparison using Student's t test).

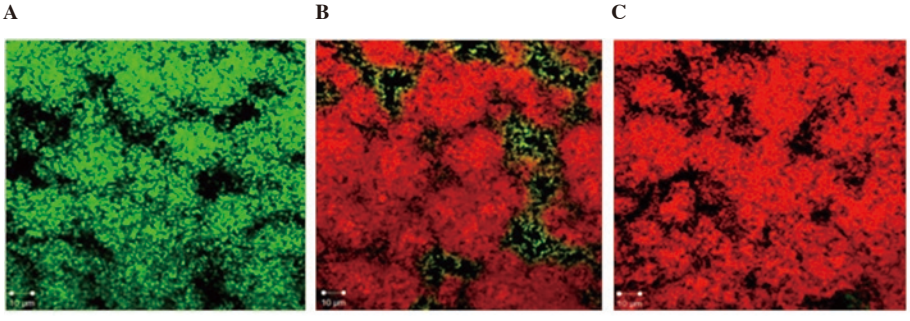

Figure 6. Confocal microscopy images of *Streptococcus mutans* biofilms grown on coverslips with AMG and nanoAMG. Biofilms of *Streptococcus mutans* were cultured for 48 h at 37 ℃ in fresh TYS medium (control) (A) or in TYS medium supplemented with 48 μmol/L AMG (B) and nanoAMG (C) (treated). The coverslips were then stained for 15 min with LIVE/DEAD BacLight mixture (50:50 v/v). Stained biofilms were observed using laser scanning confocal fluorescence microscopy (Olympus, Tokyo, Japan). The "dead" cells are in red, while "live" cells are in green. Scale bar: 10 μm.

used to prepare nanoparticles (Figure 3).

3.4. Inhibitory effect of NanoAMG on biofilm formation by S. mutans

The results presented in Figure 4A showed a remarkable reduction in biofilm biomass. At concentration ≤ 3.12 μmol/L, lower than MIC value (9.6 μmol/L, data not shown), the effects were detected with both AMG and nanoAMG. At 6.25 μmol/L, nanoAMG showed a strong inhibitory activity by reducing biofilm biomass up to 49.1% compared to 33.4% of AMG. At the concentrations of ≥ 12.5 μmol/L, biofilms in all nanoAMG treated samples were almost totally disrupted. In contrast, biofilm formation at the late stage (treated after 24 h biofilm growth) was reduced only 20.7% at 96 μmol/L (= 10 × MIC) in nanoAMG samples while almost no effect was found for AMG (Figure 4B).

3.5. NanoAMG effects on gtfB and gtfC gene expression in S. mutans biofilms

Figure 5 shows that *gtfB* gene expression levels were reduced by 2.4 and 3.3 folds for AMG and nanoAMG, respectively, while those for *gtfC* were 7.6 and 12.5 folds, respectively.

3.6. Confocal microscopy

Fluorescence appeared red, demonstrating the cells were killed by both AMG and nanoAMG, whereas green fluorescence was observed in the control sample without treatment (Figure 6).

3.7. Effect of nanoAMG on membrane permeabilization

The obtained data presented in Figure 7 indicated that nanoAMG at 12.5 μmol/L increased cell permeabilization in a time dependent manner, which was more pronounced than AMG.

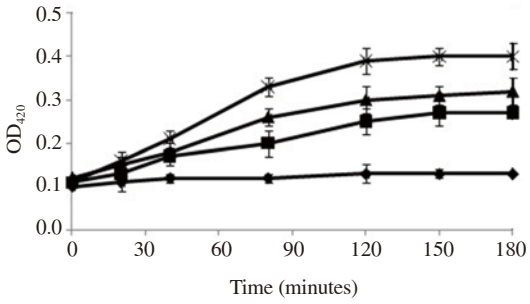

Figure 7. Effect of nanoAMG on permeabilization of the membrane of *Streptococcus mutans*. The absorbance of o-nitrophenol-β-*D*-galactoside (100 μg/mL) passage across the cytoplasmic membrane was followed at A_{420}. Control (♦); 12.5 μmol/L AMG (■); 12.5 μmol/L nanoAMG (▲); 0.5 μg/mL nisin (×) as a positive control. Data were expressed as mean ± SD (n=3).

4. Discussion

Although many phytomedicine and plant extracts possess striking potential *in vitro* bioactivities, they exhibit least or no significant *in vivo* effects due to their poor solubility, poor permeability and improper size, resulting in poor absorption and bioavailability[23]. AMG, a major compound from *G. mangostana*, is well reported for a variety of valuable bioactivities but has limited clinical application, especially in the treatment of biofilm diseases because of its high hydrophobicity, low selectivity and low bioavailability resulting from its low solubility[14,24]. To overcome these problems to make the compound as a therapeutic agent, some strategies have been made, including chemical modification, combined antibiotics/antimicrobials or nanoparticle synthesis. For modification of chemical structure, it seems not to be a successful approach since the derivatives exhibit less activity or the solubility is not always improved. Wang *et al.*[25] and Phitaktim *et al.*[21] indicated that the combination of AMG and antibiotic oxacillin can improve its antimicrobial activity against MRSA. However, it may lead to antibiotic-resistant strains, especially to oral bacteria in cariogenic biofilm, which are daily exposed to antibiotics in oral health care products. Gunasekaran *et al.*[23] suggested that nanotechnology could be an effective solution to improve AMG availability and activity. Therefore, AMG coated nanoparticles for different therapeutic purposes have been studied. Pan-In *et al.*[26,27] have successfully synthesized nanomangostin with a size of > 500 nm using ethyl cellulose as substrate and methylcellulose as carriers to treat *Propionibacterium acnes* and *Helicobacter pylori*. Yao *et al.*[28] have prepared nanoAMG using polyethylene glycol-polylactic acid as a delivery system to treat Alzheimer's disease. The polyethylene glycol-polylactic acid nanoparticles had a size of (94.26 ± 4.54) nm and zeta potential of −(32 ± 0.43) mV and improved distribution in organs such as the brain and liver. Ramadhan *et al.*[29] reported a AMG nanoemulsion using virgin coconut oil phase and mixed surfactant consisting of Tween 80 and span 80. The nanoemulsion gel penetrated the skin layer up to 12 μg/cm^2. For treatment of oral diseases, Zhou *et al.*[30] and Ren *et al.*[6] reported about cationic, pH-responsive p(DMAEMA)-*b*-p(DMAEMA-co-BMA-co-PAA) block copolymer micelles of a natural compound farnesol with high affinity for dental and biofilm surfaces and efficient anti-bacterial drug release in response to acidic pH, characteristic of cariogenic (tooth-decay causing) biofilm microenvironments. So far, the synthesis of nanoAMG for the treatment of oral bacteria biofilms related to oral diseases has not been implemented yet.

In this study, we report a new formula for preparation of polymeric nanoparticle of AMG with a size in a range of 10-50 nm, zeta potential of −35.20 mV and low polydispersity index of 0.28 that enable the agent to more easily diffuse into biofilms to reach the targets. The infrared spectrum compared to that of AMG[31] showed the stretching of the hydroxyl (-OH) band at 3 448.21 cm^{-1}, the

stretching of C=O band at 1 735.58 cm^{-1}, the stretching of C=C band at 1 637.74 cm^{-1}, and the deforming of alkyl C-H at 1 458.52, 1 351.59, and 1 250.18 cm^{-1}. The stretching of C-H band at 2 922.72, 2 875.39 cm^{-1} was consistent with the presence of methyl groups. Moreover, the spectrum exhibited a strong C-O-C band at 1 103.49 cm^{-1} compared to pure Tween 20 at 1 112.11 cm^{-1}, pure PEG 400 at 1 047 cm^{-1} and pure AMG at 1 077.13 cm^{-1}. This peak was shifted to the band of Tween 20 because its ratio was largest in the nanoAMG composition, which demonstrated that AMG was incorporated into nanoAMG. The *in vitro* data on fibroblast cells indicated that the blank carrier is safe for application, such as oral health care products, while nanoAMG cytotoxicity showed an IC_{50} value of 8.7 μg/mL. We demonstrated that the synthesized nanoAMG exhibited an improved inhibitory activity against biofilm formation by *S. mutans* compared to AMG, especially in the early biofilm stage (49.1% *vs.* 33.4%). However, the efficacy for the treatment of mature biofilms was still limited, only 20.7%. The co-delivery of AMG with other antimicrobials as a dual-targeting formula that may synergistically disrupt biofilms and kill dominant and persistently resistant cells should be tried to enhance the antibiofilm activity of the nanoAMG.

Glucosyltransferase B and C are two key enzymes responsible for extracellular polysaccharide synthesis by *S. mutans*[32]. It is known that AMG could inhibit insoluble extracellular polysaccharide synthesis by reducing enzymatic function and/or affecting transcription of the genes encoding these enzymes[13,32]. Our previous publications indicated that AMG strongly inhibited Gtfs activity responsible for exopolysaccharide production by *S. mutans*[13]. However, gene expressions were not clearly affected by this compound. In this study, using the biofilm model of 24 well plastic plates, we were able to find clear inhibition in *gtf* expression by nanoAMG. The qRT-PCR data confirm that AMG and nanoAMG inhibited biofilm formation by *S. mutans* through an inhibitory action on *gtfB* and *gtfC* at transcriptomic level in the early stage of biofilm growth. Also, the reported findings indicated that cell membrane is a primary target for damage by AMG[15,21,33]. A clear effect of the agent on *S. mutans* membrane permeabilization in this study could be additional evidence of membrane target by AMG/nanoAMG.

In conclusion, our findings suggest that the incorporation of AMG into polymer nanoparticles potentially produced better efficacy for biofilm treatment. Nevertheless, for therapeutic application, further works on *in vivo* study regarding toxicity, pharmacokinetic profiles, and bioavailability in normal subjects and those with other pathogenic bacteria still need to be characterized.

Conflict of interest statement

The authors declare that they have no competing interests.

Acknowledgments

The authors are highly appreciative of the NAFOSTED grant 106-NN.02-2016.19 for financial support. We thank A/Prof. Anh Van Thi Nguyen and Son Van Chu for help in qRT-PCR analysis, and Dr. Albert Bolhuis for help in confocal microscopy.

Funding

This work was supported by the NAFOSTED research grant 106-NN.02-2016.19 to Phuong T.M. Nguyen.

Authors' contributions

PTMN designed the project, supervised, performed the experiments, analysed data and wrote the manuscript. MTHN, LTQ, LLN and PTMN performed the experiments, and analysed data. DVQ helped in editing the manuscript. All authors have read and approved the final manuscript.

References

[1] Hall-Stoodley L, Stoodley P. Evolving concepts in biofilm infections. *Cell Microbiol* 2009; **11**(7): 1034-1043.

[2] Flemming HC, Wingender J. The biofilm matrix. *Nat Rev Microbiol* 2010; **8**: 623-633.

[3] Koo H, Allan RN, Howlin RP, Stoodley P, Hall-Stoodley L. Targeting microbial biofilms: Current and prospective therapeutic strategies. *Nat Rev Microbiol* 2017; **15**(12): 740-755.

[4] Rabin N, Zheng Y, Opoku-Temeng C, Du Y, Bonsu E, Sintim HO. Biofilm formation mechanisms and targets for developing antibiofilm agents. *Future Med Chem* 2015; **7**(4): 493-512.

[5] Benoit DSW, Sims KR Jr, Fraser D. Nanoparticles for oral biofilm treatments. *ACS Nano* 2019; **3**(5): 4869-4875.

[6] Ren Z, Kim D, Paula AJ, Hwang G, Liu Y, Li J, et al. Dual-targeting approach degrades biofilm matrix and enhances bacterial killing. *J Dent Res* 2019; **98**(3): 322-330.

[7] Sims KR, Liu Y, Hwang G, Jung HI, Koo H, Benoit DSW. Enhanced design and formulation of nanoparticles for anti-biofilm drug delivery. *Nanoscale* 2018; **11**(1): 219-236.

[8] Al-Massarani SM, El-Gamal AA, Al-Musayeib NM, Mothana RA, Basudan OA, Al-Rehaily AJ, et al. Phytochemical, antimicrobial and antiprotozoal evaluation of *Garcinia mangostana* pericarp and α-mangostin, its major xanthone derivative. *Molecules* 2013; **18**(9): 10599-10608.

[9] Nguyen PTM, Ngo VQ, Ta TM, Nguyen VA, Kuhakarn C, Reutrakul V, et al. Antibiofilm activity of α-mangostin extracted from *Garcinia*

mangostana L. against *Staphylococcus aureus*. *Asian Pac J Trop Med* 2017; **10**(12): 1154-1160.

[10]Sivaranjani M, Prakash M, Gowrishankar S, Rathna J, Pandian SK, Ravi AV. *In vitro* activity of alpha-mangostin in killing and eradicating *Staphylococcus epidermis* RP62A biofilms. *Appl Microbiol Biotechnol* 2017; **101**(8): 3349-3359.

[11]Sivaranjani M, Srinivasan R, Aravindraja C, Karutha Pandian S, Veera Ravi A. Inhibitory effect of α-mangostin on *Acinetobacter baumannii* biofilms - an *in vitro* study. *Biofouling* 2018; **234**(5): 579-593.

[12]Lemos JA, Quivey RGJr, Koo H, Abranches J. *Streptococcus mutans*: A new Gram-positive paradigm? *Microbiology* 2013; **159**(Pt 3): 436-445.

[13]Nguyen PTM, Falsetta ML, Hwang G, Gonzalez M, Koo H. α-Mangostin disrupts the development of *Streptococcus mutans* biofilms and facilitates its mechanical removal. *PLoS One* 2014; **9**(10): e111312.

[14]Aisha AF, Ismail Z, Abu-Salah KM, Majid AM. Solid dispersions of α-mangostin improve its aqueous solubility through self-assembly of nanomicelles. *J Pharm Sci* 2012; **101**(2): 815-825.

[15]Nguyen PTM, Marquis RE. Antimicrobial actions of alpha-mangostin against oral streptococci. *Can J Microbiol* 2011; **57**(3): 217-225.

[16]Rachmawati H, Novel MA, Nisa RM, Olivia GB, Tandrasasmita M, Annisa Rahma A, et ak. Antifibrotic effect of curcumin-loaded nanoemulsion and its combination with *Phaleria macrocarpa* extract to NIH 3T3 cell for antifibrosis. *J Drug Deliv Sci Technol* 2017; **39**: 123-130.

[17]Matthew AW, Franklin RC, William AC, Micheal ND, George ME, David WH, et al. Methods for dilution antimicrobial susceptibility tests for bacteria that grow aerobically. In: Lorian VS (ed.) *Clinical and laboratory standards institute document M07-A9.* Pennsylvania: Clinical and Laboratory Standards Institute; 2012, p. 16-34.

[18]Beeton ML, Aldrich-Wright JR, Bolhuis A. The antimicrobial and antibiofilm activities of copper(Ⅱ) complexes. *J Inorg Biochem* 2014; **140**: 167-172.

[19]Nguyen HT, Nguyen TT, Pham HTT, Nguyen QTN, Tran MT, Nguyen AH, et al. Fate of carotenoid-producing *Bacillus aquimaris* SH6 colour spores in shrimp gut and their dose-dependent probiotic activities. *PLoS One* 2018; **13**(12): e0209341.

[20]Alhusein N, De Bank PA, Blagbrough IS, Bolhuis A. Killing bacteria within biofilms by sustained release of tetracycline from triple-layered electrospun micro/nanofibre matrices of polycaprolactone and poly(ethylene-co-vinyl acetate). *Drug Deliv Transl Res* 2013; **3**(6): 531-541.

[21]Phitaktim S, Chomnawang M, Sirichaiwetchakoon K, Dunkhunthod B, Hobbs G, Eumkeb G. Synergism and mechanism of action of α-mangostin isolated from *Garcinia mangostana* L. and oxacillin combination against oxacillin-resistant *Staphylococcus saprophyticus*. *BMC Microbiol* 2016; **16**(1): 195.

[22]Moongkarndi P, Jaisupa N, Kosem N, Konlata J, Samer J, Pattanapanyasat K, et al. Effect of purified α-mangostin from mangosteen pericarp on cytotoxicity, cell cycle arrest and apoptotic gene expression in human cancer cells. *World J Pharm Sci* 2015; **3**(8): 1473-1484.

[23]Gunasekaran T, Haile T, Nigusse T, Dhanaraju MD. Nanotechnology: An effective tool for enhancing bioavailability and bioactivity of phytomedicine. *Asian Pac J Trop Biomed* 2014; **4**(Suppl 1): S1-S7.

[24]Chi XQ, Zi CT, Li HM, Yang L, Lv YF, Li JY, et al. Design, synthesis and structure–activity relationships of mangostin analogs as cytotoxic agents. *RSC Adv* 2018; **8**: 41377-41388.

[25]Wang M, Zhang K, Gu Q, Bi X, Wang J. Pharmacology of mangostins and their derivatives: A comprehensive review. *Chin J Nat Med* 2017; **15**(2): 81-93.

[26]Pan-In P, Tachapruetinun A, Chaichanawongsaroj N, Banlunara W, Suksamrarn S, Wanichwecharungruang S. Combating *Helicobacter pylori* infections with mucoadhesive nanoparticles loaded with *Garcinia mangostana* extract. *Nanomedicine (Lond)* 2014; **9**(3): 457-468.

[27]Pan-In P, Wongsomboon A, Kokpol C, Chaichanawongsaroj N, Wanichwecharungruang S. Depositing α-mangostin nanoparticles to sebaceous gland area for acne treatment. *J Pharmacol Sci* 2015; **129**(4): 226-232.

[28]Yao L, Gu X, Song Q, Wang X, Huang M, Hu M, et al. Nanoformulated alpha-mangostin ameliorates Alzheimer's disease neuropathology by elevating LDLR expression and accelerating amyloid-beta clearance. *J Control Release* 2016; **226**: 1-14.

[29]Ramadhan MK, Krisanti EA. Formulation and characterization of nanoemulsion gel mangosteen extract in virgin coconut oil for topical formulation. *MATEC Web Conferences* 2018; **156**: 1-7.

[30]Zhou J, Horev B, Hwang G, Klein MI, Koo H, Benoit DS. Characterization and optimization of pH-responsive polymer nanoparticles for drug delivery to oral biofilms. *J Mater Chem B* 2016; **4**(18): 3075-3085.

[31]Ahmad M, Yamin BM, Mat Lazim A. A study on dispersion and characterisation of α-mangostin loaded pH sensitive microgel systems. *Chem Cent J* 2019; **7**: 85.

[32]Bowen WH, Koo H. Biology of *Streptococcus mutans*-derived glucosyltransferases: Role in extracellular matrix formation of cariogeneic biofilms. *Caries Res* 2011; **45**(1): 69-86.

[33]Koh JJ, Qiu S, Zou H, Lakshminarayanan R, Li J, Zhou X, et al. Rapid bactericidal action of alpha-mangostin against MRSA as an outcome of membrane targeting. *Biochim Biophys Acta* 2013; **1828**(2): 834-844.

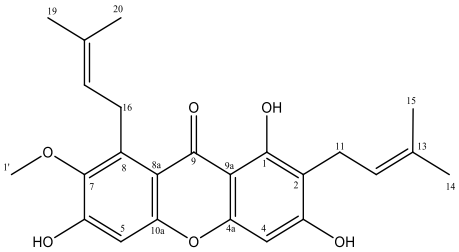

Supplementary **Figure**. Chemical structure of α-mangostin (AMG) isolated from *G. mangostana*.

Supplementary **Table**. ^{1}H and ^{13}C NMR data of AMG isolated from *Garcinia mangostana*

.

Pos.	**δ_C[a,c]**	**δ_H[a,d] (mult., *J* = Hz)**
1	159.8	-
2	109.9	-
3	162.2	-
4	92.2	6.34 (s, 1H)
4a	154.5	-
5	101.8	6.80 (s, 1H)
6	156.8	-
7	143.3	-
8	136.3	-
8a	109.6	-
9	181.2	-
9a	101.7	-
10a	154.1	-
11	20.9	3.21 (d, 2H, *J* = 7.0 Hz)
12	123.7	5.17 (t, 1H, 7.0 Hz)
13	130.3	-
14	25.4	1.62 (s, 3H)
15	17.9	1.62 (s, 3H)
16	25.5	4.02 (d, 2H, *J* = 7.0 Hz))
17	122.5	5.16 (t, 1H, 7.0 Hz)
18	130.2	-
19	25.7	1.73 (s, 3H)
20	17.6	1.77 (s, 3H)
1’	60.1	3.70 (s, 3H)
OH-1	-	13.71 (s, 1H, chelated OH)

[a]Measured in DMSO, [c]125 MHz, [d]500 MHz